Title

Source Provenance of Obsidian Artifacts from the El Paso Phase Cottonwood Springs Site (LA 175), Southern New Mexico

Author

Shackley, M. Steven

Publication Date

2014-08-11

GEOARCHAEOLOGICAL XRF LAB

GEOARCHAEOLOGICAL X-RAY FLUORESCENCE SPECTROMETRY LABORATORY
8100 WYOMING BLVD., SUITE M4-158
ALBUQUERQUE, NM 87113 USA

SOURCE PROVENANCE OF OBSIDIAN ARTIFACTS FROM THE EL PASO PHASE COTTONWOOD SPRINGS SITE (LA 175), SOUTHERN NEW MEXICO

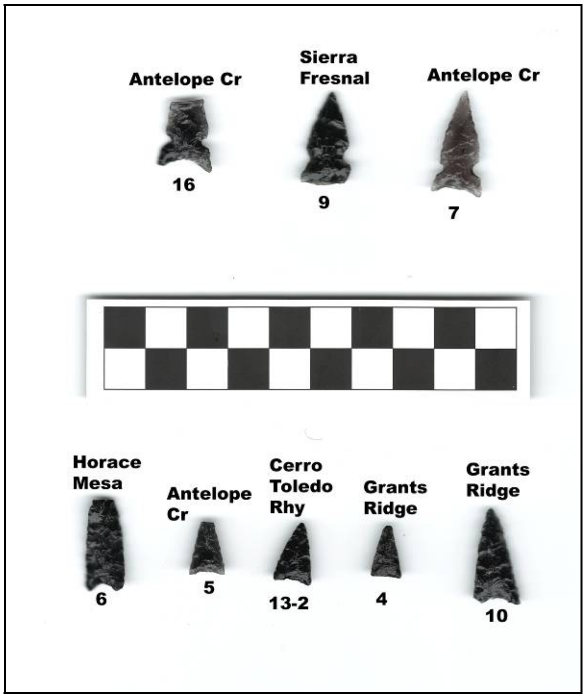

by

M. Steven Shackley Ph.D., Director
Geoarchaeological XRF Laboratory
Albuquerque, New Mexico

Report Prepared for

Sean Dolan
Department of Anthropology
University of Oklahoma, Norman

11 August 2014

INTRODUCTION

The analysis here of 40 obsidian artifacts from the Cottonwood Springs site in southern New Mexico exhibits a very diverse obsidian provenance assemblage including Jemez Mountains sources, most likely procured from Rio Grande Quaternary alluvium, Mogollon-Datil sources at Mule Creek and Nutt Mountain, and both source localities at Mount Taylor, also likely procured in Rio Grande alluvium, and Sierra Fresnal in northern Chihuahua.

LABORATORY SAMPLING, ANALYSIS AND INSTRUMENTATION

All archaeological samples are analyzed whole. The results presented here are quantitative in that they are derived from "filtered" intensity values ratioed to the appropriate x-ray continuum regions through a least squares fitting formula rather than plotting the proportions of the net intensities in a ternary system (McCarthy and Schamber 1981; Schamber 1977). Or more essentially, these data through the analysis of international rock standards, allow for inter-instrument comparison with a predictable degree of certainty (Hampel 1984; Shackley 2011).

All analyses for this study were conducted on a ThermoScientific *Quant'X* EDXRF spectrometer, located in the Archaeological XRF Laboratory, Albuquerque, New Mexico. It is equipped with a thermoelectrically Peltier cooled solid-state Si(Li) X-ray detector, with a 50 kV, 50 W, ultra-high-flux end window bremsstrahlung, Rh target X-ray tube and a 76 μm (3 mil) beryllium (Be) window (air cooled), that runs on a power supply operating 4-50 kV/0.02-1.0 mA at 0.02 increments. The spectrometer is equipped with a 200 $\mathrm{l\ min^{-1}}$ Edwards vacuum pump, allowing for the analysis of lower-atomic-weight elements between sodium (Na) and titanium (Ti). Data acquisition is accomplished with a pulse processor and an analogue-to-digital converter. Elemental composition is identified with digital filter background removal, least squares empirical peak deconvolution, gross peak intensities and net peak intensities above background.

The analysis for mid Zb condition elements Ti-Nb, Pb, Th, the x-ray tube is operated at 30 kV, using a 0.05 mm (medium) Pd primary beam filter in an air path at 200 seconds livetime to generate x-ray intensity Ka-line data for elements titanium (Ti), manganese (Mn), iron (as $Fe_2O_3^T$), cobalt (Co), nickel (Ni), copper, (Cu), zinc, (Zn), gallium (Ga), rubidium (Rb), strontium (Sr), yttrium (Y), zirconium (Zr), niobium (Nb), lead (Pb), and thorium (Th). Not all these elements are reported since their values in many volcanic rocks are very low. Trace element intensities were converted to concentration estimates by employing a least-squares calibration line ratioed to the Compton scatter established for each element from the analysis of international rock standards certified by the National Institute of Standards and Technology (NIST), the US. Geological Survey (USGS), Canadian Centre for Mineral and Energy Technology, and the Centre de Recherches Pétrographiques et Géochimiques in France (Govindaraju 1994). Line fitting is linear (XML) for all elements. When barium (Ba) is acquired in the High Zb condition, the Rh tube is operated at 50 kV and up to 1.0 mA, ratioed to the bremsstrahlung region (see Davis 2011; Shackley 2011). Further details concerning the petrological choice of these elements in Southwest obsidians is available in Shackley (1988, 1995, 2005; also Mahood and Stimac 1991; and Hughes and Smith 1993). Nineteen specific pressed powder standards are used for the best fit regression calibration for elements Ti-Nb, Pb, Th, and Ba, include G-2 (basalt), AGV-2 (andesite), GSP-2 (granodiorite), SY-2 (syenite), BHVO-2 (hawaiite), STM-1 (syenite), QLO-1 (quartz latite), RGM-1 (obsidian), W-2 (diabase), BIR-1 (basalt), SDC-1 (mica schist), TLM-1 (tonalite), SCO-1 (shale), NOD-A-1 and NOD-P-1 (manganese) all US Geological Survey standards, NIST-278 (obsidian), U.S. National Institute of Standards and Technology, BE-N (basalt) from the Centre de Recherches Pétrographiques et Géochimiques in France, and JR-1 and JR-2 (obsidian) from the Geological Survey of Japan (Govindaraju 1994).

The data from the WinTrace software were translated directly into Excel for Windows software for manipulation and on into SPSS for Windows for statistical analyses. In order to evaluate these quantitative determinations, machine data were compared to measurements of known standards during each run. RGM-1 a USGS obsidian standard is analyzed during each sample run for obsidian artifacts to check machine calibration (Table 1). Source assignments were made with reference to Shackley (1995, 2005) and source standard data at this lab (Tables 1 and 2, and Figures 1 through 3).

DISCUSSION

I've discussed the major source regions in the previous report for Lake Roberts, most of which will not be repeated here (see Shackley 2014a). There are, however, some salient points to ponder. While artifacts produced from sources that are present in Rio Grande Quaternary alluvium comprise the major component (Jemez Mountains sources of Cerro Toledo Rhyolite, Bear Springs Peak, and El Rechuelos) and Mount Taylor sources of Grants Ridge and Horace-La Jara Mesa, many of the artifacts, including projectile points were produced from obsidian that is not available in Rio Grande alluvium, including the Antelope Creek locality at Mule Creek, Nutt Mountain in Sierra County, and Sierra Fresnal in northern Chihuahua (see Table 2, and Figure 4). With regard to procurement from Rio Grande alluvial contexts, I notice many bipolar cores and flakes that exhibit waterworn cortex. Additionally, Church's (2000) study of obsidian in Rio Grande contexts in and around Las Cruces is relevant (Table 3). Interestingly, he recovered nearly the same proportion of Cerro Toledo geological obsidian as present at Cottonwood Springs (his 63%, and 62.5% here; see Tables 2 and 3). The Mount Taylor raw material was considerably greater at Cottonwood Springs at 18% to Church's 1.6%, although he recovered 12% of El Rechuelos, to only one sample at Cottonwood Springs (Church 2000; Tables 2 and 3 here).

The obsidian projectile points are typical of late period styles including concave-base, triangular forms common throughout the West, as well as what have been called Pueblo side-notched by Justice (2002) also common throughout the West, indeed most of western North America during the late periods (Turner and Hester 1985; Whittaker 1984; Figure 4 here). The source provenance of the arrowpoints also is potentially useful. All of the small concave-base, triangular points are produced from obsidian present in the Rio Grande alluvium. The nodule size is generally sufficient to produced these points, except perhaps sample numbers six and ten, although still possible. The side-notched points, however, are all produced from primary source obsidian in western New Mexico (Antelope Creek/Mule Creek) or Sierra Fresnal, northern Chihuahua. These could all have entered the Cottonwood Creek site as finished points, perhaps hafted on arrows.

As mentioned in the previous report (Shackley 2014a), the obsidian (rhyolite) sources in the Mogollon-Datil Volcanic Province of western New Mexico pose a particularly challenging problem in source discrimination for a variety of chronological and regional geological reasons (see Shackley 2014b). While Antelope Creek is easy to discriminate from the others in the province, the Gwynn/Ewe Canyon source in the Mogollon Highlands is difficult to separate from the Nutt Mountain source in Sierra County. Figure 3 is a three-dimensional plot of these two sources with the one sample (28A) that fits the Nutt Mountain elemental concentrations. The three bivariate and three-dimensional plots solve source discrimination (see also Table 1).

REFERENCES CITED

Church, T.
2000 Distribution and Sources of Obsidian in the Rio Grande Gravels of New Mexico. *Geoarchaeology* 15:649-678.

Davis, K.D., T.L. Jackson, M.S. Shackley, T. Teague, and J.H. Hampel
2011 Factors Affecting the Energy-Dispersive X-Ray Fluorescence (EDXRF) Analysis of Archaeological Obsidian. In *X-Ray Fluorescence Spectrometry (XRF) in Geoarchaeology*, edited by M.S. Shackley, pp. 45-64. Springer, New York.

Govindaraju, K.
1994 1994 Compilation of Working Values and Sample Description for 383 Geostandards. *Geostandards Newsletter* 18 (special issue).

Hampel, Joachim H.
1984 Technical Considerations in X-ray Fluorescence Analysis of Obsidian. In *Obsidian Studies in the Great Basin*, edited by R.E. Hughes, pp. 21-25. Contributions of the University of California Archaeological Research Facility 45. Berkeley.

Hildreth, W.
1981 Gradients in Silicic Magma Chambers: Implications for Lithospheric Magmatism. *Journal of Geophysical Research* 86:10153-10192.

Hughes, Richard E., and Robert L. Smith
1993 Archaeology, Geology, and Geochemistry in Obsidian Provenance Studies. *In Scale on Archaeological and Geoscientific Perspectives*, edited by J.K. Stein and A.R. Linse, pp. 79-91. Geological Society of America Special Paper 283.

Justice, N.D.
2002 *Stone Age Spear and Arrow Points of the Southwestern United States*. Indiana University Press, Bloomington.

Mahood, Gail A., and James A. Stimac
1990 Trace-Element Partitioning in Pantellerites and Trachytes. *Geochemica et Cosmochimica Acta* 54:2257- 2276.

McCarthy, J.J., and F.H. Schamber
1981 Least-Squares Fit with Digital Filter: A Status Report. In *Energy Dispersive X-ray Spectrometry*, edited by K.F.J. Heinrich, D.E. Newbury, R.L. Myklebust, and C.E. Fiori, pp. 273-296. National Bureau of Standards Special Publication 604, Washington, D.C.

Schamber, F.H.
1977 A Modification of the Linear Least-Squares Fitting Method which Provides Continuum Suppression. In *X-ray Fluorescence Analysis of Environmental Samples*, edited by T.G. Dzubay, pp. 241-257. Ann Arbor Science Publishers.

Shackley, M. Steven
1988 Sources of Archaeological Obsidian in the Southwest: An Archaeological, Petrological, and Geochemical Study. *American Antiquity* 53(4):752-772.

1990 *Early Hunter-Gatherer Procurement Ranges in the Southwest: Evidence from Obsidian Geochemistry and Lithic Technology*. Ph.D. dissertation, Arizona State University, University Microfilms, Ann Arbor.

1995 Sources of Archaeological Obsidian in the Greater American Southwest: An Update and Quantitative Analysis. *American Antiquity* 60(3):531-551.

2005 *Obsidian: Geology and Archaeology in the North American Southwest*. University of Arizona Press, Tucson.

2011 An Introduction to X-Ray Fluorescence (XRF) Analysis in Archaeology. In *X-Ray Fluorescence Spectrometry (XRF) in Geoarchaeology*, edited by M.S. Shackley, pp. 7-44. Springer, New York.

2014a Source Provenance of Obsidian Artifacts from Archaeological Sites near Lake Roberts, Southern New Mexico. Report prepared for Sean Dolan, Department of Anthropology, University of Oklahoma, Norman.

2014b Elemental and Isotopic Variability in Mogollon-Datil Volcanic Province Obsidian, Southwestern New Mexico: Issues In EDXRF Analysis. Poster presented at the International Symposium on Archaeometry, Los Angeles, California.

Turner, E.S., and T.R. Hester
1985 *A Field Guide to Stone Artifacts of Texas Indians*. Texas Monthly Press, Austin.

Whittaker, J.C.
1984 *Arrowheads and Artisans: Stone Tool Manufacture and Individual Variation at Grasshopper Pueblo*. Ph.D. dissertation, Department of Anthropology, University of Arizona, Tucson.

Table 1. Elemental concentrations and source assignments for the archaeological specimens and analysis of USGS RGM-1 obsidian standard. All measurements in parts per million (ppm).

Sample	Ti	Mn	Fe	Zn	Rb	Sr	Y	Zr	Nb	Ba	Pb	Th	Source
1	518	529	12267	137	219	9	65	184	100	n.m[1]	38	24	Cerro Toledo Rhy
2	629	480	12129	191	209	8	61	163	89	n.m	37	27	Cerro Toledo Rhy
3	656	478	12090	182	204	15	60	163	87	n.m	34	21	Cerro Toledo Rhy
4	427	797	11222	248	577	14	76	123	193	n.m	71	33	Grants Ridge/Mt Taylor
5	580	404	11807	102	252	21	39	109	26	n.m	29	33	Antelope Cr/Mule Cr
6	384	541	11370	225	512	12	92	136	222	n.m	55	26	Horace Mesa/Mt Taylor
7	741	389	11781	55	246	23	47	112	26	n.m	32	35	Antelope Cr/Mule Cr
8	306	770	10979	194	554	9	76	112	191	n.m	60	20	Grants Ridge/Mt Taylor
9	1011	306	12104	64	299	43	62	161	38	n.m	24	42	Sierra Fresnal, CHIH
10	297	685	10662	177	540	12	84	106	195	n.m	59	25	Grants Ridge/Mt Taylor
11	535	465	11743	133	202	9	60	170	97	n.m	35	27	Cerro Toledo Rhy
12	688	482	11850	134	200	8	61	171	95	n.m	35	25	Cerro Toledo Rhy
14	502	440	11610	92	196	8	66	169	97	n.m	36	27	Cerro Toledo Rhy
16	582	377	11748	81	249	20	38	114	29	n.m	29	36	Antelope Cr/Mule Cr
17	642	536	12383	150	215	8	64	176	102	n.m	39	26	Cerro Toledo Rhy
19	584	529	12430	181	225	8	64	174	103	n.m	41	31	Cerro Toledo Rhy
20	645	393	11733	107	244	21	42	108	24	n.m	29	36	Antelope Cr/Mule Cr
20	672	608	13204	236	241	9	70	181	93	n.m	50	25	Cerro Toledo Rhy
22	590	531	12325	110	219	13	68	184	102	n.m	35	30	Cerro Toledo Rhy
24	571	446	11621	120	198	8	58	162	96	n.m	32	21	Cerro Toledo Rhy
29	300	624	10637	206	498	11	75	104	182	n.m	53	18	Grants Ridge/Mt Taylor
30	550	352	9847	41	144	12	23	66	42	n.m	22	21	El Rechuelos
013-1	658	405	11824	90	263	20	44	113	25	n.m	32	40	Antelope Cr/Mule Cr
013-2	596	532	12209	150	219	11	60	171	101	n.m	36	30	Cerro Toledo Rhy
018A	512	477	11933	109	208	8	62	176	96	n.m	35	25	Cerro Toledo Rhy
018C	555	519	12416	138	220	8	64	175	98	n.m	38	27	Cerro Toledo Rhy
023A	509	396	11110	85	186	9	58	161	89	n.m	30	20	Cerro Toledo Rhy
023B	680	507	12189	170	205	10	60	168	92	n.m	35	26	Cerro Toledo Rhy
025A	542	431	11780	104	206	10	66	174	99	n.m	33	20	Cerro Toledo Rhy
025B	916	513	12950	212	217	14	64	172	93	n.m	43	20	Cerro Toledo Rhy
026A	759	368	10386	49	114	52	22	99	55	n.m	23	19	Bear Springs Pk

026B	450	804	11211	266	580	12	78	110	183	n.m	63	28	Grants Ridge/Mt Taylor
Sample	Ti	Mn	Fe	Zn	Rb	Sr	Y	Zr	Nb	Ba	Pb	Th	Source
026C	720	614	12949	189	239	8	67	173	98	n.m	44	26	Cerro Toledo Rhy
027A	486	494	11859	138	209	10	59	171	96	n.m	34	22	Cerro Toledo Rhy
027B	479	480	11983	140	209	11	63	177	96	n.m	39	22	Cerro Toledo Rhy
028A	1025	453	9220	79	198	26	30	120	22	117	22	24	Nutt Mtn
028B	758	527	12456	194	214	10	62	168	96	n.m	42	19	Cerro Toledo Rhy
028C	502	490	11884	186	201	8	56	176	92	n.m	34	24	Cerro Toledo Rhy
18B	523	525	12477	140	227	11	70	179	100	n.m	43	22	Cerro Toledo Rhy
023C	793	483	12273	173	196	10	63	158	96	n.m	35	25	Cerro Toledo Rhy
RGM1-S4	1536	275	13718	39	150	105	24	219	7	n.m	20	17	standard
RGM1-S4	1570	279	13715	38	149	107	26	218	9	n.m	23	15	standard
RGM1-S4	1572	280	13765	36	150	108	26	215	7	n.m	16	17	standard
RGM1-S4	1593	288	13228	35	148	110	20	216	7	802	19	13	standard

[1] n.m. = not measured

Table 2. Frequency distribution of obsidian source provenance.

		Frequency	Percent
Source	Cerro Toledo Rhy	25	62.5
	Antelope Cr/Mule Cr	5	12.5
	Grants Ridge/Mt Taylor	5	12.5
	Horace Mesa/Mt Taylor	1	2.5
	Bear Springs Pk	1	2.5
	El Rechuelos	1	2.5
	Nutt Mtn	1	2.5
	Sierra Fresnal, CHIH	1	2.5
	Total	40	100.0

Table 3. Frequency distribution of secondary deposit obsidian in Rio Grande alluvium near Las Cruces, New Mexico (from Church 2000:664).

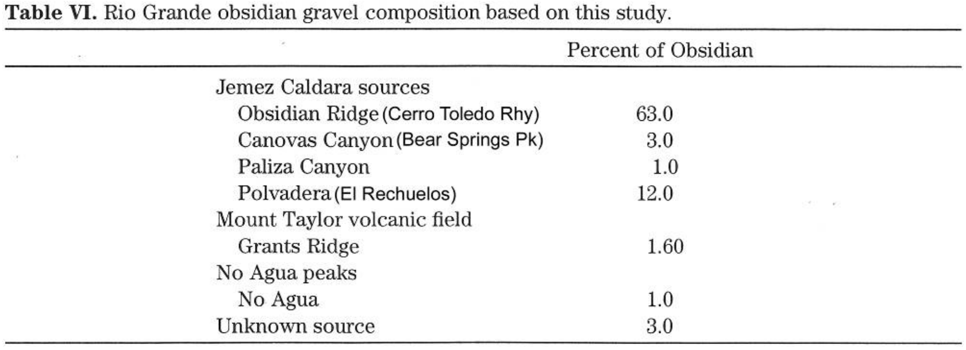

Table VI. Rio Grande obsidian gravel composition based on this study.

	Percent of Obsidian
Jemez Caldara sources	
Obsidian Ridge (Cerro Toledo Rhy)	63.0
Canovas Canyon (Bear Springs Pk)	3.0
Paliza Canyon	1.0
Polvadera (El Rechuelos)	12.0
Mount Taylor volcanic field	
Grants Ridge	1.60
No Agua peaks	
No Agua	1.0
Unknown source	3.0

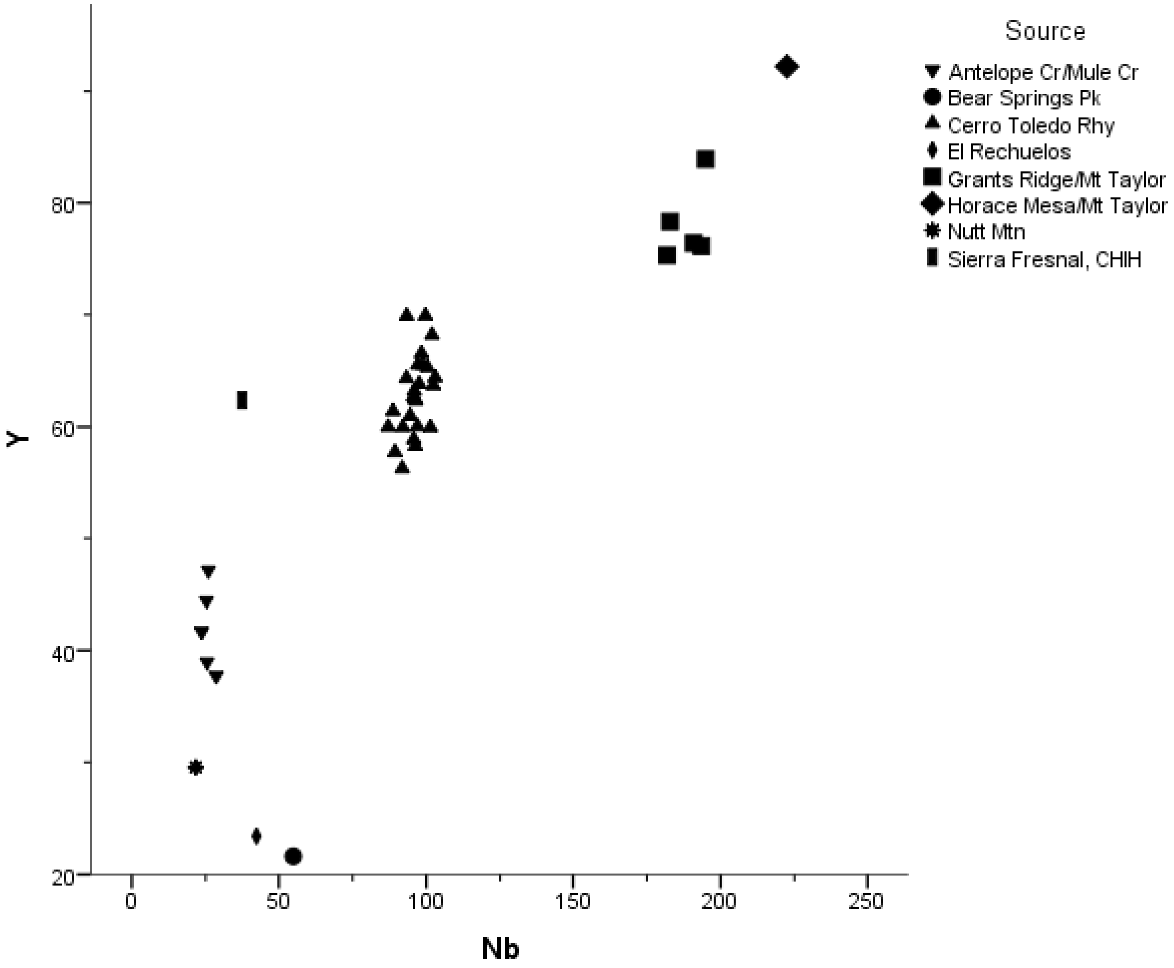

Figure 1. Nb versus Y bivariate plot of all artifacts. Following plots aid in discrimination.

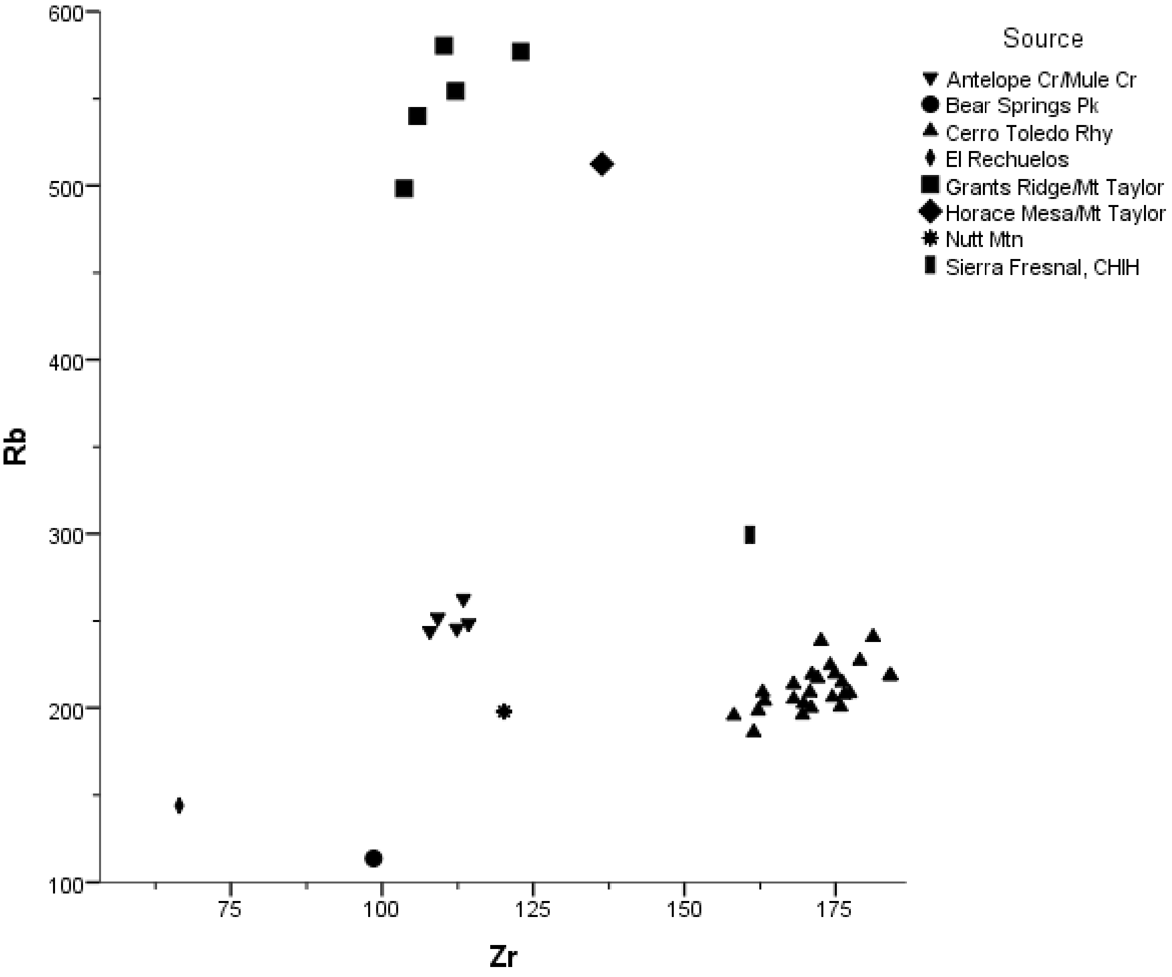

Figure 2. Zr versus Rb bivariate plot of artifacts. The Nutt Mountain, and Gwynn/Ewe Canyon samples better discriminated in the plot below.

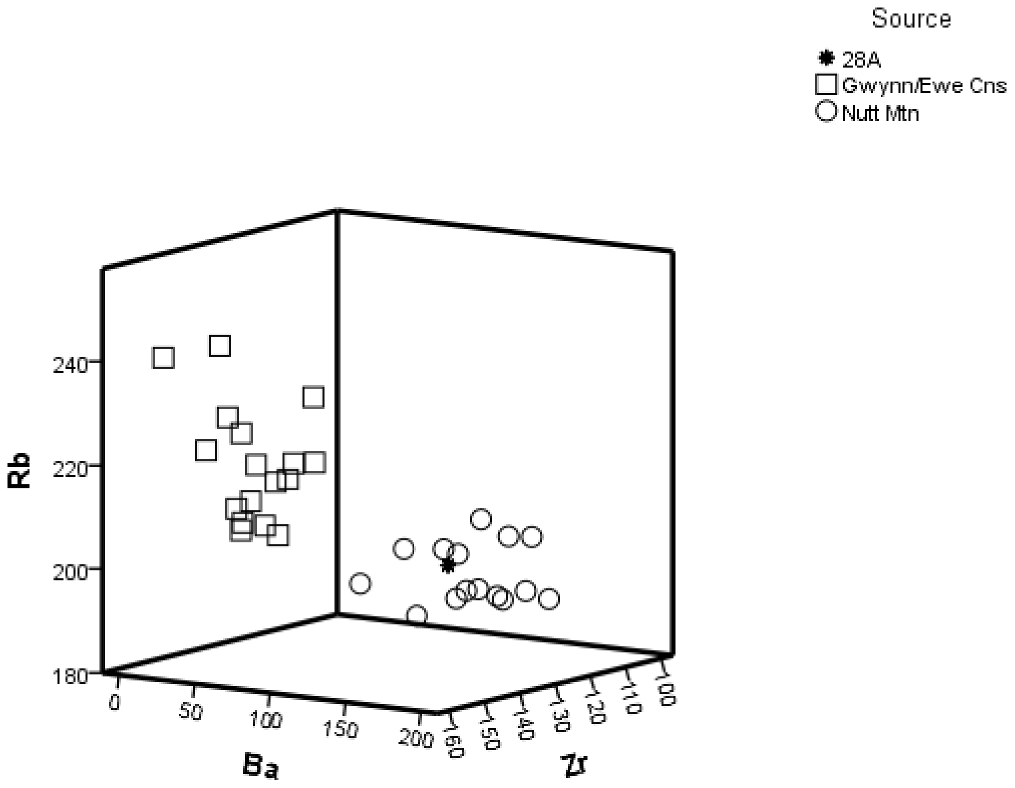

Figure 3. Ba, Rb, Zr three-dimensional plot of Gwynn/Ewe Canyon and Nutt Mountain source standards and the Gwynn/Ewe Canyon assigned artifact.

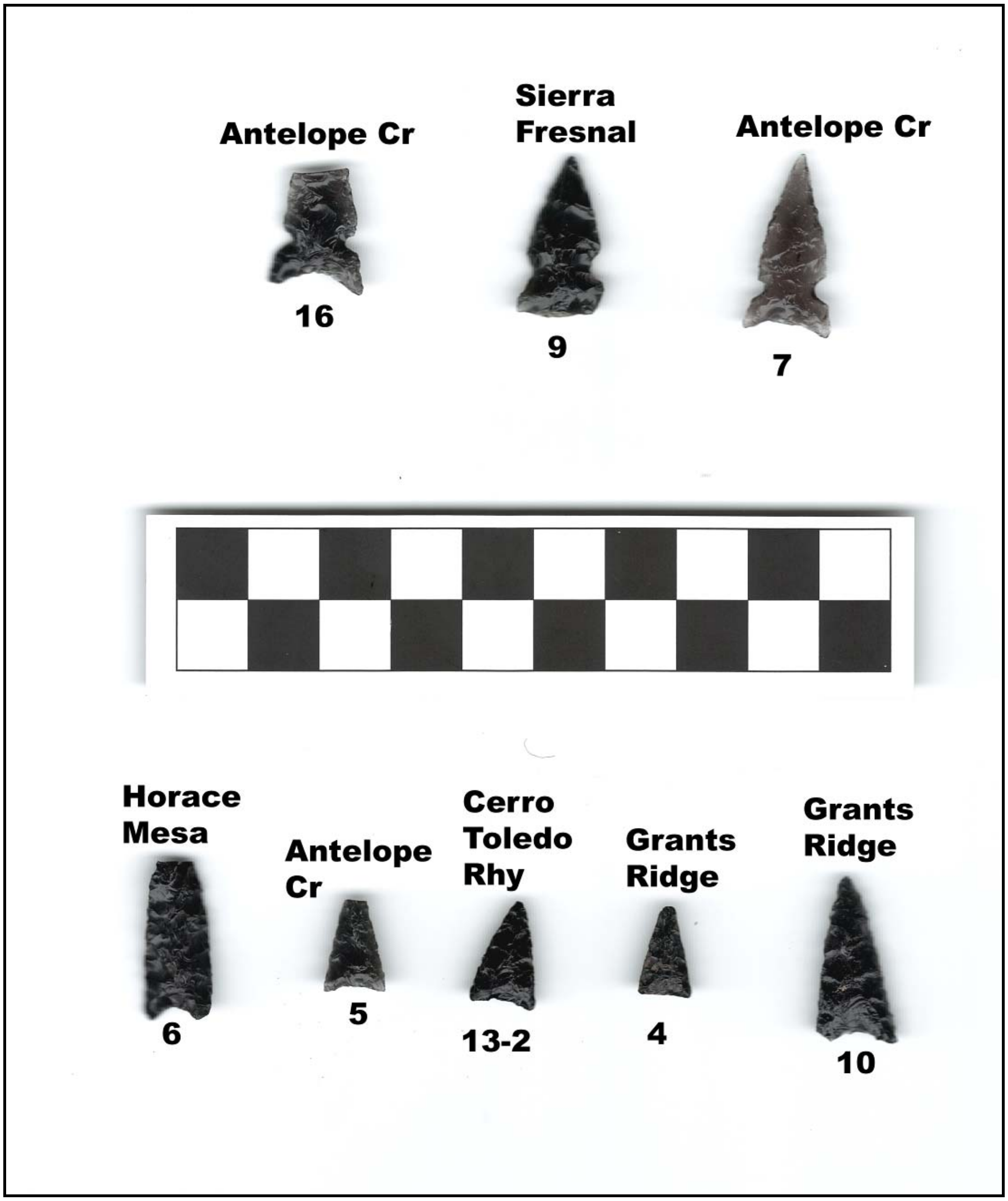

Figure 4. Selected projectile points and source assignments from the Cottonwood Creek site.